Computational Materials Science 257 (2025) 113952

Contents lists available at ScienceDirect

Computational Materials Science

journal homepage: www.elsevier.com/locate/commatsci

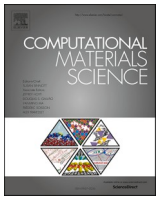

Full Length Article

First-principles prediction of the structure and stability of boron-carbon clusters

Maria Fedyaeva [a,b,*], Sergey Lepeshkin [b,c], Artem R. Oganov [b]

[a] Vernadsky Institute of Geochemistry and Analytical Chemistry, Russian Academy of Sciences, Kosygina, 19, Moscow 119991, Russia
[b] Skolkovo Institute of Science and Technology, Bolshoy Boulevard 30, bld. 1, Moscow 121205, Russia
[c] Lebedev Physical Institute, Russian Academy of Sciences, 53 Leninskii prosp., 119991 Moscow, Russia

ARTICLE INFO

Keywords:
DFT
Boron–carbon clusters
Stability
Evolutionary algorithm
Geometry classification
Building blocks
Intermediates

ABSTRACT

Boron-carbon nano-sized objects (nanoparticles, nanowires, thin films, etc.) have been actively studied in recent years for their potential applications in gas sensors, quantum dots, thermoelectric energy converters, etc. To study geometric features of these objects, we performed systematic structure prediction of B_nC_m clusters in a wide area of compositions (n, m = 0–12) using the evolutionary algorithm USPEX and first-principles calculations. We found that all obtained structures of B_nC_m clusters are planar or nearly planar and can be grouped into four classes: linear and ring-shaped structures, dense nets and nets with small holes (perforated nets). In addition, using several criteria (second-order energy differences, fragmentation energy and HOMO-LUMO gaps), we found the most stable ("magic") clusters and determined the compounds that can serve as potential building blocks or intermediates in synthesis of B-C nano-sized materials.

1. Introduction

Boron-containing clusters have recently attracted growing attention from the scientific community due to their structural complexity, unique bonding, and potential applications in nanotechnology and materials science. Among such systems, boron carbides stand out for their exceptional combination of properties, which make them the material of choice for a wide range of applications. They are distinguished by high melting point, exceptional hardness, and low specific weight. Bulk boron carbides can be used in ballistic armor, as refractory and abrasive materials, high-temperature semiconductors, ceramic materials in nanoelectronics or in flat-panel displays [1,2]. Low-dimensional B-C materials (fullerene-like nanoclusters, nanowires, nanotubes, thin films, etc.) are also actively studied in recent years. They possess even more interesting physical properties than bulk structures and may have a wider range of applications. For example, B-C nanowires demonstrated higher Seebeck coefficient and power factor than the bulk samples [3]; they are potential candidates as cathode materials [4,5]. B-C thin films are good candidates for nuclear applications due to their chemical inertness combined with the high neutron absorption capability of ^{10}B.[6] B-C nanotubes are interesting as possible drug delivery vehicle for the anticancer medicine melphalan (Mel).[7] Boron-carbon nanoclusters have gained attention due to their potential roles in the synthesis of B-C materials.[8] Therefore, determination of their atomic geometry and stability is crucial for study and modeling of the material formation processes.

Carbon and boron, despite being neighbors in the Periodic Table, exhibit distinct structural chemistries: neutral boron clusters remain planar up to B_{20},[1,9,10] while carbon clusters form linear structures up to C_9 and ring structures up to C_{18}.[11] Doping boron clusters with carbon atoms may induce structural transitions from planar to linear configurations as carbon content increases. Theoretical studies of boron–carbon clusters showed that they are characterized by structural diversity: they can be linear, ring-shaped, net-shaped, etc. For the following compositions of B − C clusters: B_nC_m (n = 0 – 5, m = 0 – 5);[12] B_nC_m (m = 1 – 4, n = 4 – 8),[13] B_4C,[14] BC_4,[15] B_nC (n = 1 – 7),[16] C_nB and C_nB_2 (n = 4 – 10),[17] B_3C_n (n = 1 – 8),[18] B_2C_4[19] and B_4C_2, [20] B_5C_n (n = 1 – 7),[18] B_nC_2 (n = 3 – 8),[21] B_8C_{10}[22] and B_nC_n (n = 1 – 13)[23] the geometries, electronic structures, bonding properties, and relative stabilities were investigated by density functional theory (DFT) calculations. As one can see, these studies were conducted for only specific compositions or small compositional ranges. Here we report a systematic investigation of stable boron–carbon B_nC_m clusters in a wide area of compositions ($0 \le n, m \le 12$) using the global optimization

* Corresponding author.
E-mail address: Maria.Fedyaeva@skoltech.ru (M. Fedyaeva).

https://doi.org/10.1016/j.commatsci.2025.113952
Received 4 February 2025; Received in revised form 27 April 2025; Accepted 27 April 2025
Available online 24 May 2025

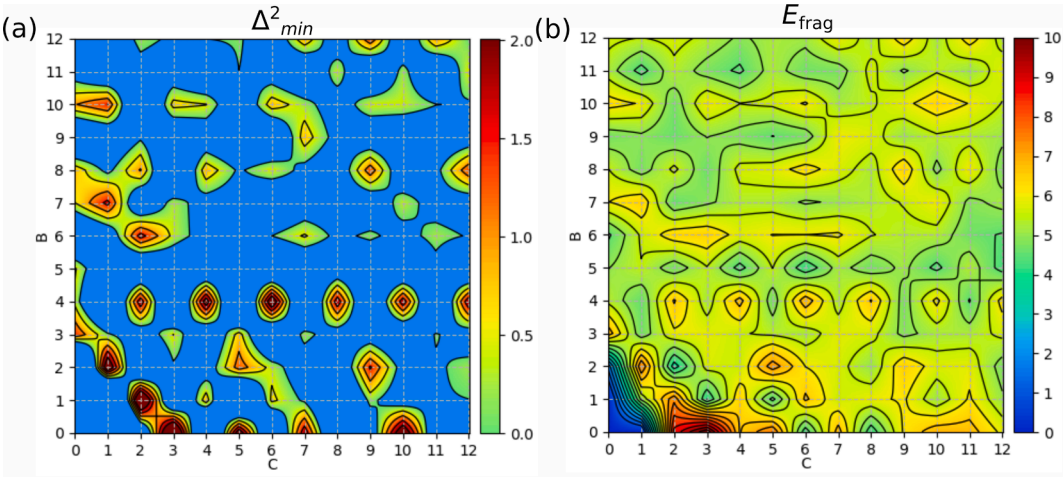

Fig. 1. Heat maps showing the stability of B_nC_m clusters using two criteria: (a) second-order differences of energy (Δ^2_{min}) and (b) fragmentation energy (E_{frag}) in eV as a function of n and m. Regions of instability are marked in blue color.

algorithm USPEX and DFT calculations. We studied their geometric and energetic characteristics, identified the most likely "magic" clusters, analyzed their geometries and identified clusters that are potential building blocks or intermediate states in chemical synthesis of more complex B-C structures. Obtained in our study stable atomic configurations can provide a foundation for comprehending the structure of B-C objects, predicting the course of chemical reactions involving them, improving existing production technologies, and explaining their growth processes in experimental settings.

2. Computational methodology

To find the most stable structures of boron–carbon clusters, we used the evolutionary algorithm USPEX [24–27] (see also http://uspex-team.org) coupled with DFT calculations. Structure relaxations were performed using the spin-polarized PBE functional [28] with the VASP code [29]. In these calculations, we used the projector augmented wave method [30] and 400 eV plane wave energy cutoff. The supercell method was employed, where periodic images of a cluster were separated by a vacuum layer with a thickness of 10 Å to ensure that the interaction between periodic images of the clusters is negligible. The final refinement was done for 25 lowest-energy isomers of each composition using the B3LYP hybrid functional [31] and 6-311 + G(d, p) basis set [32] with the Gaussian 16 [33] code. Previous studies showed that results of B3LYP/6-311G* calculations of the geometry and energetics are quite accurate and can be applied for studying of B-C clusters [14–19,34–37]. During our calculations, spin multiplicities up to 4 were checked. We also calculated the vibrational spectra for each molecule to verify dynamical stability by the absence of imaginary frequencies.

3. Results and discussion

We have found the ground-state structures of B_nC_m clusters with the number of atoms n and m from 0 to 12. The obtained structures are either identical to or more energetically favorable than those reported in previous studies: for 61 clusters, we identified the same global minima as previously found; for 16 clusters, we discovered structures with lower energy; and, to the best of our knowledge, structures for 91 compositions were predicted for the first time [8,11–23,34,38–42]. A detailed comparison between our results and literature data is given in ESI Tables S1 and S2. The geometries and energies of all clusters are given in ESI Section S1.

To study the stability of B_nC_m clusters we applied two criteria, which are often used in studies of nanoclusters [43,44]. The first one calculates second-order energy differences with respect to the number of B and C atoms (Δ^2_B (n, m) and Δ^2_C (n, m)) and takes the minimal one (Δ^2_{min} (n, m)):

$$\begin{aligned}\Delta^2_B(n,m) &= E_{n+1,m} + E_{n-1,m} - 2E_{n,m}\\ \Delta^2_C(n,m) &= E_{n,m+1} + E_{n,m-1} - 2E_{n,m}\\ \Delta^2_{min}(n,m) &= min\{\Delta^2_B(n,m); \Delta^2_C(n,m)\}\end{aligned} \quad (1)$$

where $E_{n,m}$ is the total energy of the cluster containing n boron atoms and m carbon atoms. This quantity characterizes the resistance towards the transfer of one atom of each type between two identical clusters during their collision. Clusters having a positive Δ^2_{min} are called "magic" – they are easier to form and can be obtained in higher concentrations. Previously in a series of studies it has been shown that clusters with high values of Δ^2_{min} produce higher peaks in mass spectra [45–48], which indicates their higher stability and abundance. Fig. 1a shows the heat map of $\Delta^2_{min}(n, m)$, demonstrating the existence of "islands" of stability, corresponding to the magic clusters. The compositional area of unstable clusters ($\Delta^2_{min}(n, m) < 0$) is marked in blue. In the further analysis of magic clusters we will consider $n \leq 11$ and $m \leq 11$, since for the edge compositions ($n = 12$ or $m = 12$) both second differences Δ^2_B and Δ^2_C can't be calculated together.

The second criterion is related to the calculation of the fragmentation energies for all possible fragmentation channels into two fragments $B_nC_m \rightarrow B_kC_l + B_{n-k}C_{m-l}$ with $0 \leq k \leq n$ and $0 \leq l \leq m$:

$$E_{frag}(n,m,\ k,l) = \ E(k,l) + E(n-k,m-l) - E(n,m) \quad (2)$$

among which we consider the lowest one:

$$E_{frag}(n,m) = min_{k,l}\{E_{frag}(n,m,k,l)\} \quad (3)$$

The higher E_{frag}, the more resistant the B_nC_m cluster is to fragmentation. Heat map of E_{frag} is shown on Fig. 1b. The complete set of fragmentation energies and fission products of all clusters is given in ESI Table S3. As one can see from Fig. 1, there is a noticeable correlation between the criteria related to Eq. (1) and Eq. (3). Clusters with a positive Δ^2_{min} usually have larger values of E_{frag} than those with neighboring compositions. At first glance, one can notice the following series of stable

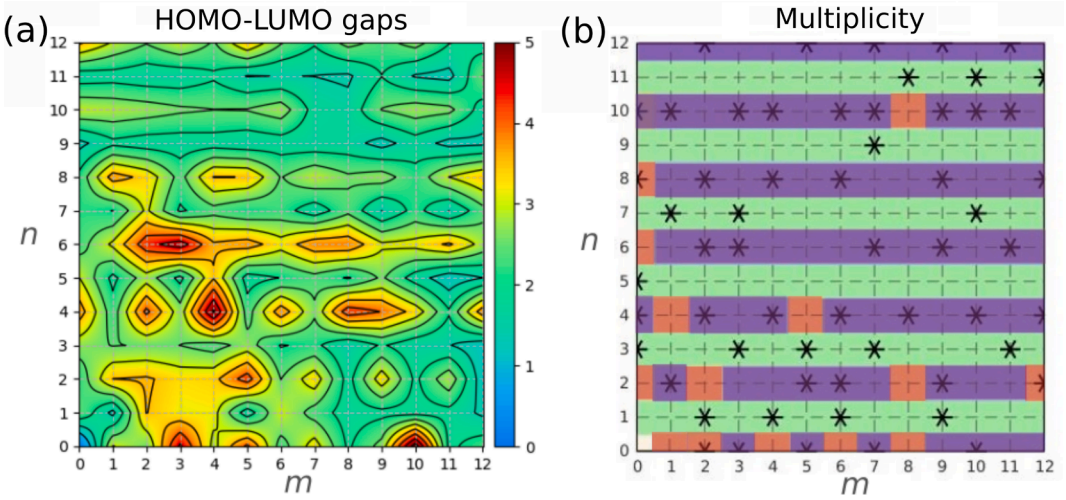

Fig. 2. Maps of a) HOMO-LUMO gaps of B_nC_m clusters (n, m = 0 – 12), b) spin multiplicities (purple – 1, green – 2, orange – 3). Magic clusters are marked with asterisks.

compositions: $B_{3-x}C_x$ ($x = 0 - 3$), B_4C_{2x} ($x = 0 - 6$), $B_{8-2x}C_{6+x}$ ($x = 0 - 4$), B_8C_{2x} ($x = 0 - 3$), $B_{10}C_{3x}$ ($x = 0 - 3$), $B_{10}C_{3x+1}$ ($x = 0 - 3$). The structures of clusters from these families are given in ESI Fig. S1.

Usually, clusters with an even total number of electrons are more stable than those with an odd number, because of the closed-shell electronic structure. In the case of B-C clusters, compositions with an odd number of boron atoms have an odd total number of electrons, while those with an even number of boron atoms – even total number of electrons. Indeed, the majority of magic B_nC_m clusters have an even number of B atoms, the best example of which is the B_4C_{2x} series (x = 0–6). However, there are cases where clusters with an odd number of electrons are also magic, which may result from a closed structural shell. This is observed in clusters of pure boron (B_3 and B_5) and is in agreement with literature .[41] We also found many magic binary B_nC_m clusters with an odd number of electrons: B_1C_2, B_1C_6, B_3C_3, B_3C_7, B_3C_{11}, B_7C_1, B_7C_{10}, B_9C_7, $B_{11}C_8$.

To evaluate the effects of temperature, we recalculated the corresponding stability maps at temperatures of 500 K and 1000 K (see ESI Fig. S2), using the Gibbs free energy instead of the internal energy in Eqs. (1-3). The overall features of the landscapes remained nearly unchanged.

We also calculated the energy gaps between highest occupied and lowest unoccupied molecular orbitals (HOMO–LUMO gaps, E_g) of the B_nC_m clusters and drew the corresponding heat map (see Fig. 2a). As electronic polarization is related to excitation of electrons into unoccupied levels, the HOMO-LUMO gap characterizes the polarizability of clusters. Large HOMO–LUMO gap is often related to closed-shell electronic structure and relatively high chemical inertness, both of which are indicative of stability. Indeed, as we can see from Fig. 1a, 1b and 2a, the behavior of $E_g(n, m)$ roughly correlates with $\Delta^2_{\min}(n, m)$ and $E_{\text{frag}}(n, m)$, which means that we can use HOMO-LUMO gaps as an indirect indicator of clusters' stability.

We also plotted the map of the optimal spin multiplicities of B_nC_m clusters (n, m = 0–12). Clusters with an even number of electrons have possible multiplicities of 1 or 3 (see Fig. 2b), whereas clusters with an odd number of electrons have only multiplicity of 2 (multiplicity of 4 is energetically unfavorable). From the literature, it is already known that a multiplicity of 3 is characteristic for some pure boron (B_2, B_6, B_8) and carbon clusters (C_2, C_4, C_6, C_8) [11]. In the current work, we have also found a number of B-C clusters with a preferable multiplicity of 3: B_2C_2,

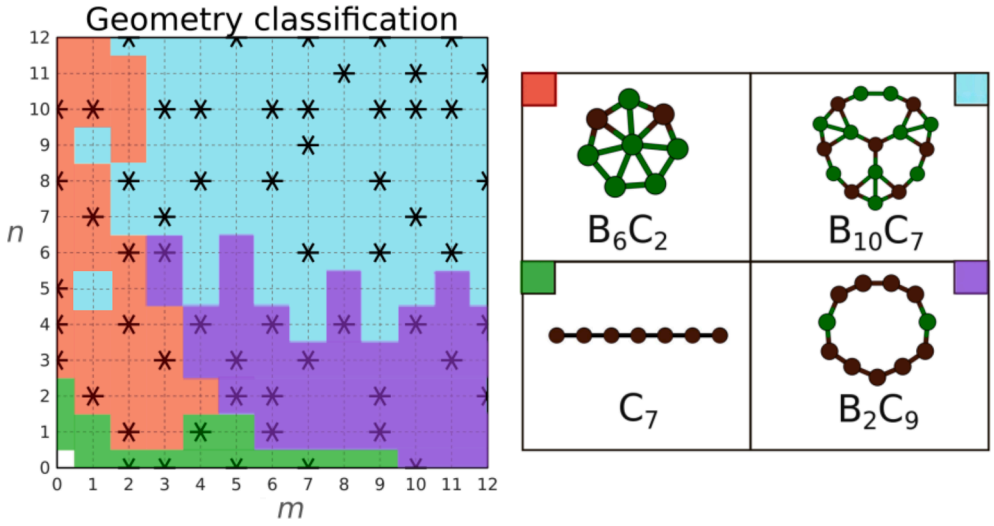

Fig. 3. Geometric classification map of B_nC_m (n, m = 0 – 12) clusters, on which clusters with different types of structures are shown in various colors: linear – green, ring-shaped – purple, dense nets – red, perforated nets – blue. Magic clusters are marked with asterisks. On the right side, examples of clusters of each geometry type are provided. Boron (B) is marked by green, carbon (C) – by brown color.

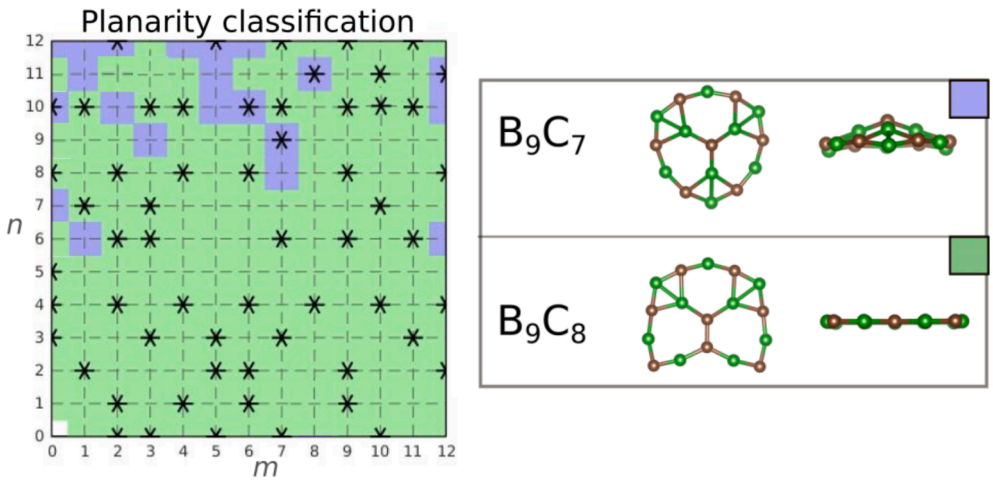

Fig. 4. Planarity classification map of B_nC_m (n, m = 0 – 12) clusters, on which clusters with different types of structures are shown in various colors: planar – green, non-planar – purple. Magic clusters are marked with asterisks. On the right side, examples of planar and non-planar clusters are provided. Boron (B) is marked by green, carbon (C) – by brown.

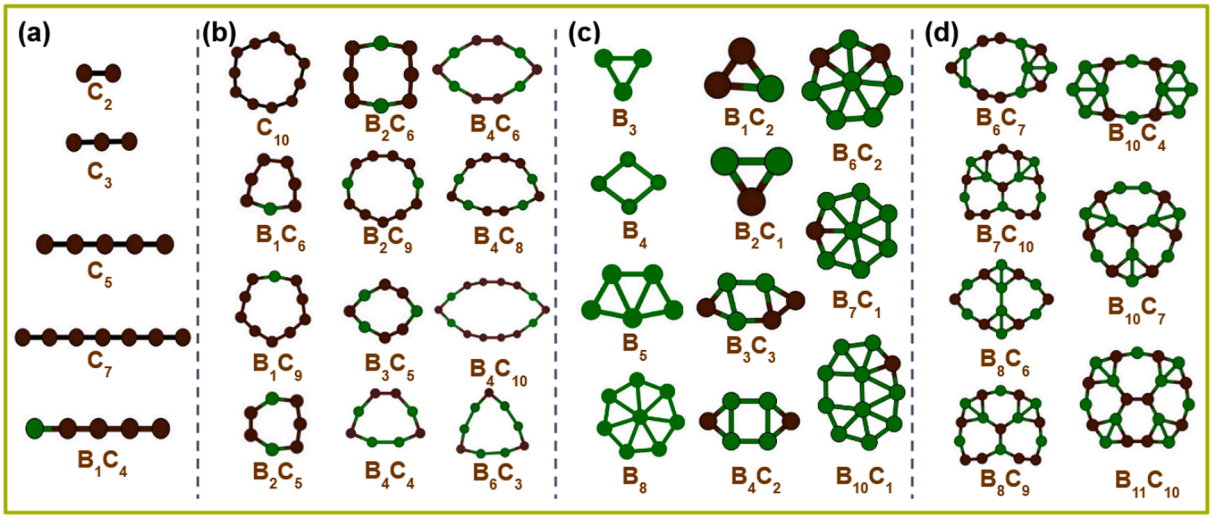

Fig. 5. Structures of B_nC_m clusters (n, m = 0 – 12), which are potential intermediate particles during synthesis processes: (a) linear, (b) ring shaped, (c) dense nets and (d) perforated nets or building blocks for nano-sized B-C structures: (c) dense nets and (d) perforated nets. Boron (B) is marked by green, carbon (C) – by brown.

B_2C_8, B_2C_{12}, B_4C_1, B_4C_5, $B_{10}C_8$, however, none of them are magic.

Next, a detailed analysis of the geometric features of B-C clusters was conducted. Considering ground-state structures of B_nC_m clusters in the whole compositional area (n, m = 0–12), we identified four main geometry types: linear and ring-shaped structures, dense nets and nets with holes (perforated nets). Fig. 3 displays a map on which clusters with different geometry types are marked by different colors: linear clusters (rods) are marked by green, ring-shaped by purple, dense and perforated nets – by red and blue, respectively. Rings have closed structure, which makes them more inert and less prone to react. In contrast, rods have at least two terminal atoms, which makes them highly reactive – they can significantly modify their structure upon interacting with other particles. Both rods and rings, due to their geometry, apparently can't fill space densely. On the contrary, dense and perforated nets may fill the space without large voids. That is why they are more suitable as building blocks of larger nanoformations. In addition, perforated nets attract additional interest due to the possibility of their doping (placing extra atoms in the holes) and the resulting creation of new magnetic 2D materials.

We also inspected the planarity of all obtained clusters. Fig. 4 shows a compositional map on which planar and non-planar clusters are highlighted by different colors (green for planar and purple for non-planar). We found that the majority of clusters in the studied region are planar, while non-planar structures are generally located in compositional area with a large number (>8) of boron atoms. However, no clear relationship between the clusters' stoichiometry and their planarity was established. For example, the B_9C_8 cluster is planar, while the neighboring B_9C_7 cluster possesses non-planar structure, resembling a cap (see Fig. 4). Thinking about using the B_nC_m clusters as building blocks, one can suggest that planar ones are more favorable. Filling the space by non-planar clusters can lead to larger stresses in the resulting larger structures, adversely affecting their stability and likelihood of formation.

The performed classification is crucial from the standpoint of determination of building blocks (dense and perforated nets) or intermediate states (all types of structures) for the synthesis of more complex B-C formations. Our final analysis identified clusters that are particularly suitable for this purpose: they should be magic and possess planar structures. Further we selected configurations with higher symmetry because usually they are more energetically favorable and are prefered in nature and in synthetic systems. The chosen clusters are shown in Fig. 5: C_2, C_3, C_5, C_7, B_1C_4 (linear, Fig. 5a), C_{10}, B_1C_6, B_1C_9, B_2C_5, B_2C_6,

B_2C_9, B_3C_5, B_4C_4, B_4C_6, B_4C_8, B_4C_{10}, B_4C_{12} (ring shaped, Fig. 5b), $B_{10}C_1$, B_7C_1, B_6C_2, B_4C_2, B_3C_3, B_2C_2, B_2C_1, B_1C_2 (dense nets, Fig. 5c), $B_{11}C_{10}$, $B_{10}C_6$, B_8C_{12}, B_8C_9, B_8C_6, B_7C_{10}, B_6C_3 (perforated nets, Fig. 5d).

4. Conclusions

We have predicted the atomic structures of B_nC_m clusters in a wide range of compositions (n, $m = 0 – 12$) using the evolutionary algorithm USPEX and DFT calculations. The stability of all clusters was determined using two main criteria: the second-order energy difference (Δ^2E) and fragmentation energy (E_{frag}), and was presented in the form of heat maps. Preferable multiplicities and HOMO-LUMO gap values were also determined for each cluster, which can be used in further studies of magnetic and optical properties. We analyzed the atomic structures of all obtained clusters: found planar/non-planar geometries and identified four main geometry types – linear, ring-shaped, dense and perforated nets. As a result, we have proposed the set of clusters, which, due to their energetic and geometric properties, may serve as building blocks or intermediate states in the chemical synthesis of complex B-C formations. The diverse structural motifs and stability patterns revealed in this study can serve as a foundation for the design of novel boron–carbon-based nanostructures. These findings may also facilitate the exploration of larger clusters, charged species, doped systems, or assemblies with specific target properties, making them promising candidates for future applications.

CRediT authorship contribution statement

Maria Fedyaeva: Writing – original draft, Visualization, Validation, Investigation, Formal analysis. **Sergey Lepeshkin:** Writing – review & editing, Software, Methodology, Data curation, Conceptualization. **Artem R. Oganov:** Writing – review & editing, Supervision, Resources, Project administration, Funding acquisition.

Declaration of competing interest

The authors declare that they have no known competing financial interests or personal relationships that could have appeared to influence the work reported in this paper.

Acknowledgments

Global structure optimization was supported by the Russian Science Foundation (Grant 19-72-30043). The calculations were performed on Oleg and Arkuda supercomputers at Skoltech and at the Joint Supercomputer Center of the Russian Academy of Sciences. The stability analysis was performed within the Project of the State Assignment (Vernadsky Institute of Geochemistry and Analytical Chemistry of Russian Academy of Sciences, Moscow, Russia).

Appendix A. Supplementary material

Supplementary data to this article can be found online at https://doi.org/10.1016/j.commatsci.2025.113952.

Data availability

The authors declare that all other data supporting the findings of this study are available within the paper and its supplementary information files.

References

[1] K.M. Reddy, P. Liu, A. Hirata, T. Fujita, M.W. Chen, *Nat. Commun.*, 4 (2013) 2483.
[2] S. Song, W. Xu, R. Cao, L. Luo, M.H. Engelhard, M.E. Bowden, B. Liu, L. Estevez, C.-M. Wang, J.-G. Zhang, *Nano Energy* 33 (2017) 195–204.
[3] K. Kirihara, M. Mukaida, Y. Shimizu, *Nanotechnology* 28 (2017) 145404.
[4] Y. Huang, F. Liu, Q. Luo, Y. Tian, Q. Zou, C. Li, C. Shen, S. Deng, C. Gu, N. Xu, H. Gao, Nano Res. **5** (2012) 896–902.
[5] V. Gokul, M. S. Swapna, V. Raj, H. V. Saritha Devi, S. Sankararaman, Int. J. Thermophys., DOI:10.1007/s10765-021-02859-0.
[6] A.O. Sezer, J.I. Brand, Mater. Sci. Eng. B Solid State Mater. Adv. Technol., 79 (2001) 191–202.
[7] F. Abolhasani Zadeh, S. Abdalkareem Jasim, M. Javed Ansari, D. Olegovich Bokov, G. Yasin, L. Thangavelu, M. Derakhshandeh, *J. Mol. Liq.*, 354 (2022) 118796.
[8] A.S. Sharipov, B. I. Loukhovitski, A.M. Starik, Eur. Phys. J.D., DOI:10.1140/epjd/e2015-60308-0.
[9] B. Kiran, S. Bulusu, H.-J. Zhai, S. Yoo, X.C. Zeng, L.-S. Wang, *Proc. Natl. Acad. Sci. USA* 102 (2005) 961–964.
[10] C. Romanescu, D.J. Harding, A. Fielicke, L.-S. Wang, *J. Chem. Phys.*, 137 (2012) 014317.
[11] S.V. Lepeshkin, V.S. Baturin, A.S. Naumova, A.R. Oganov, *J. Phys. Chem. Lett.*, 13 (2022) 7600–7606.
[12] A. S. Sharipov, B. I. Loukhovitski and A. M. Starik, *Eur. Phys. J. D*, , DOI:10.1140/epjd/e2015-60308-0.
[13] Y. Pei, X.C. Zeng, *J. Am. Chem. Soc.* 130 (2008) 2580–2592.
[14] C. Liu, M. Tang, H. Wang, *J. Phys. Chem. A* 111 (2007) 704–709.
[15] A.M. McAnoy, J.H. Bowie, S.J. Blanksby, *J. Phys. Chem. A* 107 (2003) 10149–10153.
[16] R. Wang, D. Zhang, R. Zhu, C. Liu, *THEOCHEM* 817 (2007) 119–123.
[17] K. Chuchev, J.J. BelBruno, *J. Phys. Chem. A* 108 (2004) 5226–5233.
[18] C. Wang, W. Cui, J. Shao, X. Zhu, X. Lu, *Int. J. Quantum Chem.*, 113 (2013) 2514–2522.
[19] J. Shao, C. He, R. Shi, C. Wang, X. Zhu, X. Lu, *THEOCHEM* 961 (2010) 17–28.
[20] C. He, J. Shao, R. Shi, X. Zhu, *Comput Theor. Chem.*, 967 (2011) 59–66.
[21] C. Wang, W. Cui, J. Shao, X. Zhu, X. Lu, *Comput Theor. Chem.* 1006 (2013) 19–30.
[22] S.-J. Lu, *Chem. Phys. Lett.*, 801 (2022) 139715.
[23] X. Chen, C. Zhang, B. Song, P. He, *Mater. Res Express* 7 (2020) 015041.
[24] S.V. Lepeshkin, V.S. Baturin, Y.A. Uspenskii, A.R. Oganov, *J. Phys. Chem. Lett.*, 10 (2019) 102–106.
[25] A.O. Lyakhov, A.R. Oganov, H.T. Stokes, Q. Zhu, *Comput. Phys. Commun.*, 184 (2013) 1172–1182.
[26] A.R. Oganov, A.O. Lyakhov, M. Valle, *Acc. Chem. Res.*, 44 (2011) 227–237.
[27] A.R. Oganov, C.W. Glass, *J. Chem. Phys.*, 124 (2006) 244704.
[28] J.P. Perdew, K. Burke, M. Ernzerhof, *Phys. Rev. Lett.*, 77 (1996) 3865–3868.
[29] G. Kresse, J. Furthmüller, *Phys. Rev. B Condens. Matter* 54 (1996) 11169–11186.
[30] P.E. Blöchl, *Phys. Rev. B Condens. Matter* 50 (1994) 17953–17979.
[31] M.E. Casida, C. Jamorski, K.C. Casida, D.R. Salahub, *J. Chem. Phys.*, 108 (1998) 4439–4449.
[32] P.J. Stephens, F.J. Devlin, C.F. Chabalowski, M.J. Frisch, *J. Phys. Chem.*, 98 (1994) 11623–11627.
[33] M.J. Frisch, G.W. Trucks, H.B. Schlegel, G.E. Scuseria, M.A. Robb, J.R. Cheeseman, G. Scalmani, V. Barone, G.A. Peters-son, H. Nakatsuji, X. Li, M. Caricato, A.V. Marenich, J. Bloino, B.G. Janesko, R. Gomperts, B. Mennucci, H.P. Hratchian, J.V. Ortiz, A.F. Izmaylov, J.L. Sonnenberg, D. Williams-Young, F. Ding, F. Lipparini, F. Egidi, J. Goings, B. Peng, A. Petrone, T. Henderson, D. Ranasinghe, V.G. Zakrzewski, J. Gao, N. Rega, G. Zheng, W. Liang, M. Hada, M. Ehara, K. Toyota, R. Fukuda, J. Hasegawa, M. Ishida, T. Nakajima, Y. Honda, O. Kitao, H. Nakai, T. Vreven, K. Throssell, J.A. Montgomery, Jr., J.E. Peralta, F. Ogliaro, M.J. Bearpark, J.J. Heyd, E.N. Brothers, K.N. Kudin, V.N. Staroverov, T.A. Keith, R. Kobayashi, J. Normand, K. Raghavachari, A.P. Ren-dell, J.C. Burant, S.S. Iyengar, J. Tomasi, M. Cossi, J.M.Millam, M. Klene, C. Adamo, R. Cammi, J.W. Ochterski, R.L. Martin, K. Morokuma, O. Farkas, J.B. Foresman, D.J. Fox, Gaussian 16 Revision C.01, Gaussian Inc., Wallingford CT, 2016.
[34] C. Liu, P. Han, M. Tang, Rapid Commun. Mass Spectrom. 25 (2011) 1315–1322.
[35] I.A. Popov, V.F. Popov, K.V. Bozhenko, I. Černušák, A.I. Boldyrev, *J. Chem. Phys.*, 139 (2013) 114307.
[36] Bull. Korean Chem. Soc. **26** (2005) 63–71.
[37] L.-M. Wang, B.B. Averkiev, J.A. Ramilowski, W. Huang, L.-S. Wang, A.I. Boldyrev, *J. Am. Chem. Soc.*, 132 (2010) 14104–14112.
[38] R.B. Woodward, F.E. Bader, H. Bickel, A.J. Frey, R.W. Kierstead, *J. Am. Chem. Soc.*, 78 (1956) 2023–2025.
[39] K. Wang, S.-J. Lu, C.-B. Zhang, Theor. Chem. Acc., DOI:10.1007/s00214-022-02885-7.
[40] S.S. Ray, R.K. Sahoo, S. Sahu, in: International conference on multifunctional materials (ICMM-2019), AIP Publishing, 2020.
[41] I. Boustani, *Phys. Rev. B Condens. Matter* 55 (1997) 16426–16438.
[42] B.T. Truong, D.J. Grant, M.T. Nguyen, D.A. Dixon, *J. Phys. Chem. A* 114 (2010) 994–1007.
[43] A. Arab, M. Habibzadeh, *J. Nanostructure Chem.*, 6 (2016) 111–119.
[44] Z. Hashemi, S. Rafiezadeh, R. Hafizi, S.J. Hashemifar, H. Akbarzadeh, *Chem. Phys. Lett.*, 698 (2018) 41–50.
[45] X.-P. Li, W.-C. Lu, Q.-J. Zang, G.-J. Chen, C.Z. Wang, K.M. Ho, *J. Phys. Chem. A* 113 (2009) 6217–6221.
[46] C. Rajesh, C. Majumder, M.G.R. Rajan, S.K. Kulshreshtha, Phys. Rev. B Condens. Matter Mater. Phys., DOI:10.1103/physrevb.72.235411.
[47] C.P. Poole Jr, F.J. Owens, *Introduction to Nanotechnology*, John Wiley & Sons, 2003.
[48] Y. Wang, Y. Zhou, Y. Zhang, W.E. Buhro, *Inorg. Chem.*, 54 (2015) 1165–1177.